RSC Advances

PAPER

View Article Online
View Journal | View Issue



Cite this: *RSC Adv.*, 2026, **16**, 12383

# The pH-dependence of copper(II/I) reduction potentials in variants of *P. aeruginosa* azurin with surface histidine variations

Sara Ghodrati Dolatshamloo, Nikta Ghazi and Jeffrey J. Warren *

Proteins that mediate redox transformations almost always display a degree of pH dependence in their reduction potentials. It is appreciated that surface charges can influence the physical properties of embedded sites. Less clear is the role that the distance between pH-sensitive (titratable) surface sites and embedded metal ions plays in regulating redox reactions. Here, we explore how the distance between pH-sensitive histidine sites and the copper ion in *Pseudomonas aeruginosa* azurin influences the pH dependence of the Cu(II)/Cu(I) reduction potential. Pourbaix diagrams were constructed for six azurin variants and effective p$K_a$ values for the oxidized and reduced forms of the proteins were determined. While the reduction potentials are mostly insensitive to the locations of the histidine amino acid substitutions, the effective p$K_a$ values do change. There is little correlation with the histidine-copper distance, and a more significant correlation with the histidine–histidine distance. The results support that redox-dependent protonation of amino acid sites is coupled to both the long-range electrostatic interactions of embedded cofactors and to other ionisable amino acid residues.

Received 22nd December 2025
Accepted 23rd February 2026

DOI: 10.1039/d5ra09911k

rsc.li/rsc-advances



## Introduction

More often than not, aqueous reduction potentials are pH dependent, or 'proton-coupled'. The pH dependence is often tightly coupled and a Nernstian E/pH relationship is observed, as is the case for small biomolecules like quinones, phenols (tyrosine) and flavins.[1–3] However, many redox-active proteins (*e.g.*, metalloproteins) also show pH-dependent reduction potentials, but those potentials do not typically show a simple $nH^+/ne^-$ relation. Some examples include copper,[4,5] heme,[6,7] and iron-sulphur cluster proteins.[8,9] The factors that influence the behaviours of embedded metal sites have long been known to be diverse,[10,11] and it is clear that charges at protein surfaces are one of the key factors. In this work, we explore how solution pH affects Cu(II)/Cu(I) reduction potentials in azurin (Az) variants where titratable histidine residues are introduced at different protein surface sites.

The protein Az is a prototypical member of the large class of "blue copper" electron transfer proteins.[12–14] This family of proteins has distinct physical properties that support their functions as biological electron carriers and mediators of redox reactions. Az's folded stability, tolerance to amino acid substitutions, and ease of recombinant expression have made it a useful model for the investigation of a wide range of chemical and biochemical properties.[12–15] Of particular importance are the many investigations of its intermolecular and intramolecular redox reactions.[16–18] The literature examples are too numerous to list, so the above citations are for a few key review articles. Herein, we investigate the pH-dependent redox properties of Az variants where histidine (His) amino acid residues are placed at six different surface sites of the Az structure.

The pH dependence of the Az Cu(II)/Cu(I) redox couple has been extensively investigated, including in other single amino acid substituted variants.[4,5] Azurin's reduction potential exhibits a well-characterized pH dependence, which has been attributed mainly to the protonation states of two non-coordinating, surface exposed His residues: H83 and H35.[4,5] NMR[19,20] and electrochemical[5,21] studies have shown that H35, located ~8 Å from the copper site, undergoes protonation after electron transfer, when the copper centre becomes reduced (Cu(II) → Cu(I)). H83 is somewhat more solvent exposed and farther from the Cu ion (*i.e.*, ~12 Å from the copper centre). These residues account for nearly all the measured charge regulation in azurin, as indicated by both experimental and computational analyses.

The pH-dependent redox behaviour of wild type (WT) Az has been modelled using a proton-coupled thermodynamic framework (Scheme 1), yielding effective p$K_a$ values of 6.26 (in the oxidized, or Cu(II), form) and 7.31 (in the reduced, or Cu(I), form).[5] The scheme follows conventions used in thermochemical 'square schemes' that are discussed in detail elsewhere.[1–3] The combined protonation effects of H83 and H35 can lead to reduction potential shifts of up to 60 mV over the physiological pH range. This behaviour has been explored computationally,[22]

*Department of Chemistry, Simon Fraser University, 8888 University Drive, Burnaby, BC V5A 1S6, Canada. E-mail: jjwarren@sfu.ca*

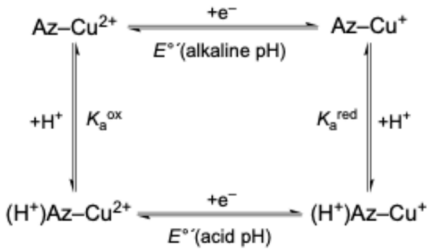


Scheme 1 Proton-coupled reaction scheme for the pH dependence of the azurin copper(II/I) formal reduction potentials ($E°'$).

and more recently, the degree to which both H35 and H83 change p$K_a$ with respect to the oxidation state of the Cu ion was investigated with experiment and theory.[23,24] Ultimately, the role of these residues in affecting Cu reduction potentials provides a basis for rational engineering of charge-sensitive redox properties in Az.

Given the well-known influence of distance on the rates of electron transfer reactions in Az,[17,18] we rationalized that Az variants with different distances between a titratable histidine and the Cu ion would display an analogous distance dependence. Given that replacement of H35 has a negligible effect on the Cu ion,[4] we opted to employ variants where H35 was constant and other histidine sites were introduced at known locations in Az.[17,18] The pH dependence of the Cu(II)/Cu(I) reduction potentials in six Az variants is explored below.

## Materials and methods

Additional experimental details and data are provided in the SI. Plasmids encoding for each Az variant were prepared using an established polymerase chain reaction and the primers used are set out in the SI. Each of the known Az variants were expressed and purified to homogeneity. Mass spectrometry and UV-visible spectroscopy protein characterization data that confirm production of each Az variant are provided in the SI (Fig. S1–S7).

Electrochemical measurements were carried out using a standard 3-electrode cell with a basal plane graphite (BPG) working electrode,[25] a platinum counter electrode, and a silver/silver chloride (saturated KCl) reference electrode. Potentials were calibrated with respect to cobalt(II)tris(2,2′-bipyridyl) $(PF_6)_2$ at all pH values. Acetate-phosphate-borate (APB) buffer was used for each experiment. The APB buffer composition was: 20 mM sodium acetate, 20 mM sodium phosphate, 20 mM sodium borate, and 100 mM potassium chloride. Protein concentrations were 30 μM for all electrochemistry experiments. In cyclic voltammetry (CV) measurements, the scan rate was 50–100 mV $s^{-1}$. Differential pulse voltammetry (DPV) data were collected at 3 mV increments with 50 mV pulse amplitude, 50 ms pulse width, 16.7 ms sample width, and 500 ms pulse period. All electrochemistry experiments used 2 s quiet time prior to data collection. Peak-to-peak separations for CV were between 100 and 150 mV, in agreement with previous observations for Az in solution.[26,27] The full width at half maximum for the DPV scans was 108 ± 5 mV across all pH values, which is close to the theoretical limit for reversible couples (90.4 mV).[28]

GROMACS[29] was used for simulations with the charmm36m[30] forcefield port.[31] Starting from the X-ray coordinates for Az (PDB ID 4AZU[21]), the A-chain was selected for simulations. Forcefield parameters for the Cu site were taken from the literature.[32] Following solvation and ionic strength adjustment, the system was equilibrated for temperature and pressure.[33] For each protein, 15 ns simulations were carried out. Clusters were identified using the gromos algorithm[34] with a 0.115 nm cutoff and using the last 4 ns of the simulations. RMSD and RMSF plots for all simulations are shown in the SI.

## Results and discussion

A series of known Az variants were prepared from the wild-type (WT) plasmid.[35] Site-directed mutagenesis was used to produce plasmids encoding for the following amino acid substitutions: H83Q, H83Q/Q107H, H83Q/M109H, H83Q/K122H, H83Q/T124H, and H83Q/T126H. As noted above, these variants have been used in studies of long-range electron transfer reactions.[36,37] Importantly, these amino acid variations do not affect the structure or the properties of the Az copper active site.[27,38–42] Successful expression and purification was confirmed using MALDI mass spectrometry and UV-visible (UV-vis) spectroscopy. In accord with past reports, the optical spectra are unaltered by the replacement of surface sites with histidine. This is an indication that the Cu site is not affected by surface substitutions, *i.e.*, as characteristic cysteine112-copper charge transfer band at 628 nm is the same as WT Az.

Electrochemical data were collected as described above. Both the cyclic voltammetry (CV) and the differential pulse voltammetry (DPV) techniques were explored. In both cases, the values of the Cu(II)/Cu(I) couples were in line with many past studies of other Az variants, including solution measurements and graphite-adsorbed Az.[4,5,26,43–45] While the CV data were clearest at low pH waves (pH 4–5), at pH > 6, the redox waves were subsumed by background currents and any correction proved unsatisfactory. Some representative electrochemical data are shown in the SI (Fig. S8). In contrast, DPV scans yielded clear, reproducible peaks with symmetric shapes (an indication of reversibility), so the DPV technique was used to collect the data

Table 1 Summary of reduction potential and p$K$ values for Az variants[a]

| Variant | $E_{low}$ | $E_{high}$ | p$K_{ox}$ | p$K_{red}$ |
|---|---|---|---|---|
| WT[5] | 0.349 | 0.292 | 7.31 | 6.26 |
| H83Q | 0.346 | 0.288 | 6.98 | 5.98 |
| H83Q/Q107H | 0.349 | 0.288 | 7.07 | 6.07 |
| H83Q/M109H | 0.348 | 0.278 | 7.01 | 5.79 |
| H83Q/K122H | 0.349 | 0.279 | 7.16 | 5.98 |
| H83Q/T124H | 0.336 | 0.273 | 7.11 | 6.02 |
| H83Q/T126H | 0.334 | 0.276 | 6.86 | 5.88 |

[a] Errors associated with $E$ values are ± 5 mV with respect to scan-to-scan variability and the error on the p$K$ fits was ±0.07 (95% confidence). The p$K$ values are from fits to eqn (1).

between pH 4 and 9, as shown in Table 1 and in Fig. 1. The errors associated with electrochemical measurements are ±5 mV with respect to scan-to-scan variability. We note that the potentials obtained from CV scans between pH 4 and 5 corroborate the values obtained from DPV.

The collected DPV data (Fig. 1) were analysed using the established $E^{o\prime}$-pH relation for Az and its variants (eqn (1)):[4,5]

$$E^{o\prime}(\mathrm{pH}) = E^{o\prime}(\text{low pH}) + \frac{RT}{nF}\ln\left(\frac{K_a^{red} + [H^+]}{K_a^{red} + [H^+]}\right) \quad (1)$$

where $E^{o\prime}$ (pH) is the observed formal potential at a given pH, $E^{o\prime}$ (low pH) is the formal potential (pH independent) at acidic pH values, $R$ is the universal gas constant, $T$ is temperature, $n$ is the number of electrons involved in the redox process, $F$ is the Faraday constant, the respective $K_a$ values correspond to the net ionization constants of the oxidized and reduced protein states and $[H^+]$ is the proton concentration at a given pH value. The $E_{low}$ values were fixed at the measured values at *ca.* pH = 4 for each variant.

The p$K$ values from nonlinear least squares analysis of the data in Fig. 1 using eqn (1) are set out in Table 1, along with known data for WT Az. The error associated with the p$K$ values for each fit (95% confidence bounds) was ±0.07 p$K$ units. First, the low and high pH reduction potentials are similar (344 ± 7 mV), as are the low pH values (282 ± 7 mV). As such, the $\Delta E$ values also are similar (62 ± 6 mV). The values are very nearly within error of each other, which is perhaps not surprising given the single amino acid variations. The small size of the Az protein means that all single-site His variations are less than about 26 Å of the Cu ion. The p$K$ values from fits to eqn (1) show a similarly low degree of variability, with fit p$K_{red}$ values of 5.99 ± 0.15 and p$K_{ox}$ values of 7.06 ± 0.15. The average $\Delta$p$K$ value is 1.07 ± 0.09. Note that the above errors are one standard deviation of the mean.

To gain more insight into the Az structures and any local interactions that can influence His p$K_a$ values, we carried out molecular dynamics (MD) simulations and used the equilibrated structures to estimate p$K_a$ values. Examples of local interactions around each histidine are set out in the SI (Fig. S9–S21). The RMSF and RMSD plots for each simulation are shown in the SI (Fig. S22–S23). Using the gromos-identified cluster structures, the DeepKa[46,47] algorithm was used to estimate p$K_a$ values of H35 and the other variant His sites, as well as the protein isoelectric points (pI). The results are tabulated in the SI (Table S1). Unfortunately, the calculated p$K_a$ values differ from experimental values, although they are in an appropriate range. The pI values are lower than the reported value of 5.6.[48] With respect to the p$K$ values, in the oxidized from of Az, the p$K_a$ value for H35 has been reported to be around 6.[49] The corresponding values for His83 is about 7.5.[26,27] This is, in terms of magnitudes, opposite the calculation. We think that the discrepancy between experiment and theory is likely due to exclusion of the Cu ion. Correlations between experimental and calculated p$K$ values are shown in the SI (Fig. S24).

The structures from MD simulations also provide a more realistic view of distances between protein locations. To a first approximation, the degree of 'interaction' between the Cu ion and the surface His site can be described by the physical distance between the sites. This is the basis for both approaches to rationalizing electron transfer kinetics[36,37] and for understanding distant electrostatic interactions in proteins.[50–53] With respect to Az, there exists great deal of research into

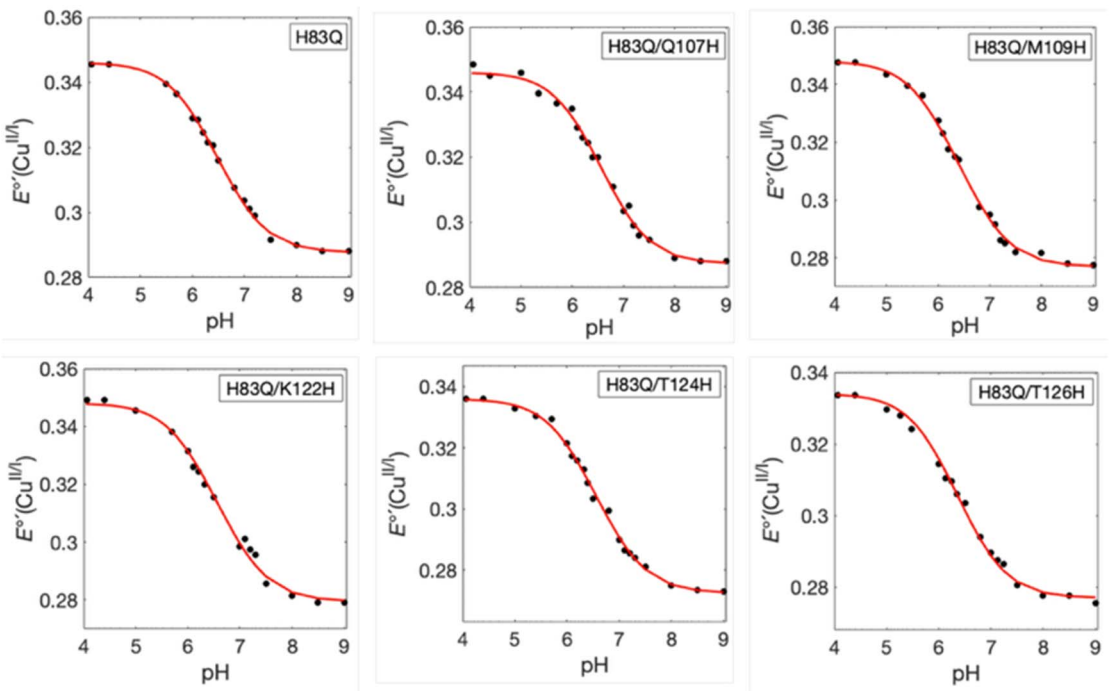


Fig. 1 Pourbaix diagrams for the six Az variants studied here. The solid red line is a fit to eqn (1). The $E^{o\prime}$ values are referenced to SHE.

intramolecular electron transfer in proteins, including but not limited to Az.[17,18,54,55] Importantly, the Az-histidine variants presented here are directly connected to the Cu ion *via* a continuous β-strand, either *via* the M121 of the C112 Cu ion ligands. The exception is H83, but this residue is in a privileged site where the electronic coupling to the Cu ion is strong.[56,57]

Again, using the MD structure clusters, the average distance (in Å) from the histidine ring centroid to the Az-Cu ion were determined and the values are set out in Table 2. To our surprise, there was no obvious correlation between the distances and any of the experimental p$K$ or $E$ values (Table 1). Plots showing these correlations (or lack thereof) are shown in the SI (Fig. S25–S28). For example, using either a distance dependence for electron transfer model or the distant-dependent Coulomb-like model, there is no correlation with the p$K_{ox}$ or p$K_{red}$ values. There is, of course, no correlation with the reduction potentials at high and low pH since they are nearly the same within experimental error.

So far, the focus has been on how the redox properties of the Az-Cu ion are influenced by the location of the histidine sites. However, there also exist examples of the influence of two or more charged sites on each other's properties.[51,53] In Staphylococcus nuclease (a non-redox protein), replacement of anionic amino acid residues (glutamate or aspartate) with cationic (lysine) or neutral (alanine) induces marked shifts in p$K_a$ values of histidine sites in a distance dependent manner. The idea is supported by theoretical approaches[50] and by combined experiment/theory analysis of protein p$K_a$ values.[58] Likewise, studies of heme proteins also show a distance dependence on electrostatic interactions of charged hemes.[51]

Plots of p$K_{ox}$ and p$K_{red}$ as a function of histidine–histidine distance (*i.e.*, the ring centroid of H35 to the ring centroid of H$X$, where $X$ = 83, 107, 109, 122, 124, or 126) show a roughly linear correlation (Fig. 2). The correlation is much stronger for the p$K_{red}$ values, where the Cu site is overall neutral in charge. This is likely because in the oxidized state (formally Cu(II)) the active site bears a net +1 charge. Due to the locations of the two histidine sites (H35 and H$X$), this effectively places the Cu ion between the two residues. Note that the above citations describing the distance dependence of charge–charge interactions use different forms of the Poisson–Boltzmann equation and Coulomb's law to rationalize interactions. The models are not strictly linear, but the distances considered here are too large to present any curvature, which is more commonly observed at distances shorter than 10 Å. In the end, the placement of the histidine sites appear to have a greater effect on one another than they do on the pH dependence and overall reduction potentials of the Cu ion in Az.

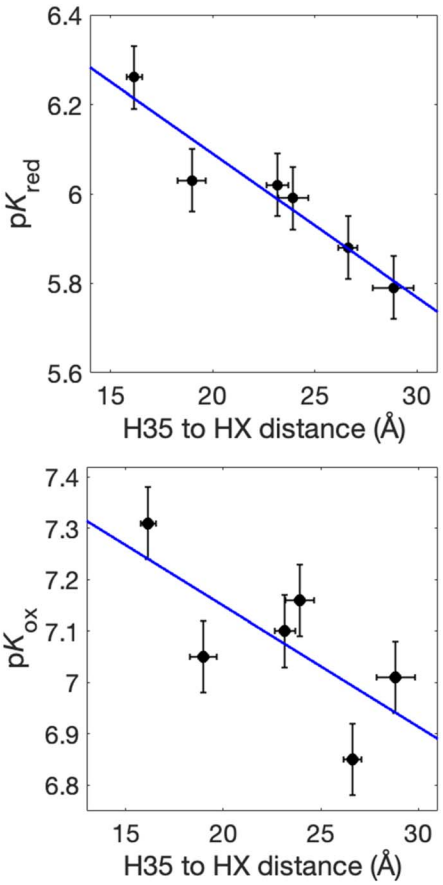


Fig. 2 Correlations of p$K_{ox}$ and p$K_{red}$ values with the histidine–histidine distances in Az variants. The distance metrics are given by the two centroids of the histidine imidazole rings.

Table 2 Distance metrics for histidine Az variants

| Variant | $d$ (H$X$–Cu)[a] | $d$ (H35–H$X$)[a] |
|---|---|---|
| WT | 14.1 ± 0.4 | 16.2 ± 0.4 |
| H83Q | 7.5 ± 0.1[b] | N/A |
| H83Q/Q107H | 23.1 ± 0.4 | 28.8 ± 1.0 |
| H83Q/M109H | 16.3 ± 0.3 | 23.9 ± 0.7 |
| H83Q/K122H | 12.3 ± 0.4 | 19.0 ± 0.7 |
| H83Q/T124H | 18.4 ± 0.4 | 23.2 ± 0.5 |
| H83Q/T126H | 21.4 ± 0.4 | 26.6 ± 0.5 |

[a] distances are averages and standard deviations (in Å) from MD simulations. [b] Crystallographic average from PDB ID 4AZU.[21]

## Conclusions

The pH dependence of the Az Cu(II/I) reduction potential was investigated in six variant proteins where the native H35 was held invariant and other histidine sites were systematically introduced around the protein. The Az Cu(II/I) reduction potentials themselves are nearly independent of the site(s) of histidine in the Az variants studied. Using a known model that describes the pH dependence of $E^{o\prime}$(Cu(II/I)) in Az, effective p$K_a$ values for the oxidized and reduced proteins were determined. The changes in effective p$K_a$ values are sensitive to the location of the histidine sites, but they do not show an obvious correlation with histidine-Cu distance. However, there exists a weak linear correlation with the p$K$ values for the reduced (Cu(I)) proteins if the histidine–histidine distances are considered. An even weaker correlation exists for the oxidized (Cu(II)) proteins, but in this case the Cu ion lies between the two histidine sites. Thus, our results suggest that the long-range electrostatic

interaction between the two histidine sites could play a large role in affecting each other's properties, and the charge on the Cu ion adds another layer of influence, especially in the oxidized protein. The network of electrostatic interactions that mutually influence protein p$K$ and $E$ values is clearly complex and more work is still needed in this area.

The weak influence of the histidine variants on the overall pH dependence of the Az reduction potentials is worth comment. The resilience of function in proteins with amino acid variations has been commented on with respect to 'compensating' electrostatic interactions.[59] The idea also has been proposed with respect to evolutionary changes in cytochrome c oxidase proteins.[60] Based on our results, we proposed that H35 is able to more (or less) compensate for the natural pH dependence of Az in such a way that the variant proteins exhibit behaviours that are very similar to the wild type protein. This is supported by the fact that variants at H35 (while retaining H83) show a pH-dependence that is the same as for the wild-type protein.[4] It also is interesting to note that smaller p$K_{red}$ values occur when (i) H35 is the only ionisable histidine (*i.e.*, the H83Q variant), when the two His are farthest apart (*e.g.*, H83Q/T126H), and when a cationic site is replaced with histidine (*i.e.*, H83Q/K122H). However, the correlation is not perfect; the H83Q/Q107H variant is an outlier. We think that much more work is needed to fully understand the interplay of redox reactions (and active site charge) and protonation state of surface sites in proteins. The idea that charge regulation can be tied to the outer-sphere reorganization energy in redox proteins[23,24] is one example of how proton-coupled electron transfer reactions can play unexpected roles in biological redox reactions. Developing further understanding of how long-range electrostatic interactions influence biological redox reactions is similarly important.

## Author contributions

Conceptualization: JJW; formal analysis: SGD, NG, JJW; funding acquisition: JJW; investigation: SGD, NG, JJW; methodology: SGD, NG, JJW; project administration: JJW; resources: JJW; supervision: JJW; writing – original draft: SGD, NG, JJW; writing – final draft: SGD, NG, JJW.

## Conflicts of interest

There are no conflicts to declare.

## Data availability

The data supporting this article have been included as part of the supplementary Information (SI). Supplementary information is available. See DOI: https://doi.org/10.1039/d5ra09911k.

## Acknowledgements

We acknowledge financial support from the Natural Sciences and Engineering Research Council of Canada (NSERC, RGPIN 06272) and from Simon Fraser University. The computational efforts here were enabled by support provided by the Digital Research Alliance of Canada (alliancecan.*ca*)

## References

1 J. J. Warren, T. A. Tronic and J. M. Mayer, *Chem. Rev.*, 2010, **110**, 6961–7001.
2 R. G. Agarwal, C. F. Wise, J. J. Warren and J. M. Mayer, *Chem. Rev.*, 2022, **122**, 1482.
3 R. G. Agarwal, S. C. Coste, B. D. Groff, A. M. Heuer, H. Noh, G. A. Parada, C. F. Wise, E. M. Nichols, J. J. Warren and J. M. Mayer, *Chem. Rev.*, 2022, **122**, 1–49.
4 T. Pascher, B. G. Karlsson, M. Nordling, B. G. Malmström and T. Vänngård, *Eur. J. Biochem.*, 1993, **212**, 289–296.
5 C. S. St. Clair, W. R. Ellis and H. B. Gray, *Inorg. Chim. Acta*, 1992, **191**, 149–155.
6 F. A. Leitch, G. R. Moore and G. W. Pettigrew, *Biochemistry*, 1984, **23**, 1831–1838.
7 G. R. Moore, G. W. Pettigrew, R. C. Pitt and R. J. P. Williams, *Biochim. Biophys. Acta*, 1980, **590**, 261–271.
8 Y. Zu, J. A. Fee and J. Hirst, *J. Am. Chem. Soc.*, 2001, **123**, 9906–9907.
9 Y. Zu, M. M.-J. Couture, D. R. J. Kolling, A. R. Crofts, L. D. Eltis, J. A. Fee and J. Hirst, *Biochemistry*, 2003, **42**, 12400–12408.
10 D. C. Rees, *Proc. Natl. Acad. Sci. U.S.A.*, 1985, **82**, 3082–3085.
11 G. R. Moore, G. W. Pettigrew and N. K. Rogers, *Proc. Natl. Acad. Sci. U.S.A.*, 1986, **83**, 4998–4999.
12 H. B. Gray, B. G. Malmström and R. J. P. Williams, *J. Biol. Inorg. Chem.*, 2000, **5**, 551–559.
13 J. J. Warren, K. M. Lancaster, J. H. Richards and H. B. Gray, *J. Inorg. Biochem.*, 2012, **115**, 119–126.
14 J. Liu, S. Chakraborty, P. Hosseinzadeh, Y. Yu, S. Tian, I. Petrik, A. Bhagi and Y. Lu, *Chem. Rev.*, 2014, **114**, 4366–4469.
15 E. I. Solomon, D. E. Heppner, E. M. Johnston, J. W. Ginsbach, J. Cirera, M. Qayyum, M. T. Kieber-Emmons, C. H. Kjaergaard, R. G. Hadt and L. Tian, *Chem. Rev.*, 2014, **114**, 3659–3853.
16 O. Farver and I. Pecht, *J. Am. Chem. Soc.*, 1992, **114**, 5764–5767.
17 H. B. Gray and J. R. Winkler, *Chem. Phys. Lett.*, 2009, **483**, 1–9.
18 H. B. Gray and J. R. Winkler, *Q. Rev. Biophys.*, 2003, **36**, 341–372.
19 A. P. Kalverda, M. Ubbink, G. Gilardi, S. S. Wijmenga, A. Crawford, L. J. C. Jeuken and G. W. Canters, *Biochemistry*, 1999, **38**, 12690–12697.
20 G. W. Canters, H. A. O. Hill, N. A. Kitchen and E. T. Adman, *Eur. J. Biochem.*, 1984, **138**, 141–152.
21 H. Nar, A. Messerschmidt, R. Huber, M. van de Kamp and G. W. Canters, *J. Mol. Biol.*, 1991, **221**, 765–772.
22 R. T. Ullmann and G. M. Ullmann, *J. Phys. Chem. B*, 2011, **115**, 10346–10359.
23 C. T. Zahler, H. Zhou, A. Abdolvahabi, R. L. Holden, S. Rasouli, P. Tao and B. F. Shaw, *Angew. Chem., Int. Ed.*, 2018, **57**, 5364–5368.

24 C. T. Zahler and B. F. Shaw, *Chem. Eur. J.*, 2019, **25**, 7581–7590.
25 S. S. Hanson and J. J. Warren, *Can. J. Chem.*, 2017, **96**, 119–123.
26 S. M. Berry, M. H. Baker and N. J. Reardon, *J. Inorg. Biochem.*, 2010, **104**, 1071–1078.
27 J. J. Warren, N. Herrera, M. G. Hill, J. R. Winkler and H. B. Gray, *J. Am. Chem. Soc.*, 2013, **135**, 11151–11158.
28 A. J. Bard and L. R. Faulkner, *Electrochemical Methods: Fundamentals and Applications*, John Wiley and Sons, New York, 2nd edn, 2001.
29 M. J. Abraham, T. Murtola, R. Schulz, S. Páll, J. C. Smith, B. Hess and E. Lindahl, *SoftwareX*, 2015, **1–2**, 19–25.
30 J. Huang, S. Rauscher, G. Nawrocki, T. Ran, M. Feig, B. L. de Groot, H. Grubmüller and A. D. MacKerell, *Nat. Methods*, 2017, **14**, 71–73.
31 A. F. Wacha and J. A. Lemkul, *J. Chem. Inf. Model.*, 2023, **63**, 4246–4252.
32 V. Rajapandian, V. Hakkim and V. Subramanian, *J. Phys. Chem. B*, 2010, **114**, 8474–8486.
33 J. A. Lemkul, *J. Phys. Chem. B*, 2024, **128**, 9418–9435.
34 X. Daura, K. Gademann, B. Jaun, D. Seebach, W. F. van Gunsteren and A. E. Mark, *Angew. Chem., Int. Ed.*, 1999, **38**, 236–240.
35 T. K. Chang, S. A. Iverson, C. G. Rodrigues, C. N. Kiser, A. Y. Lew, J. P. Germanas and J. H. Richards, *Proc. Natl. Acad. Sci. U.S.A.*, 1991, **88**, 1325–1329.
36 R. Langen, I.-J. Chang, J. P. Germanas, J. H. Richards, J. R. Winkler and H. B. Gray, *Science*, 1995, **268**, 1733–1735.
37 J. J. Regan, A. J. Di Bilio, R. Langen, L. K. Skov, J. R. Winkler, H. B. Gray and J. N. Onuchic, *Chem. Biol.*, 1995, **2**, 489–496.
38 A. J. Di Bilio, B. R. Crane, W. A. Wehbi, C. N. Kiser, M. M. Abu-Omar, R. M. Carlos, J. H. Richards, J. R. Winkler and H. B. Gray, *J. Am. Chem. Soc.*, 2001, **123**, 3181–3182.
39 A. M. Blanco-Rodriguez, M. Busby, C. Gradinaru, B. R. Crane, B. Di, P. Matousek, M. Towrie, B. S. Leigh, J. H. Richards, A. Vlcek and H. B. Gray, *J. Am. Chem. Soc.*, 2006, **128**, 4365–4370.
40 C. Shih, A. K. Museth, M. Abrahamsson, A. M. Blanco-Rodriguez, A. J. Di Bilio, J. Sudhamsu, B. R. Crane, K. L. Ronayne, M. Towrie, A. Vlcek, J. H. Richards, J. R. Winkler and H. B. Gray, *Science*, 2008, **320**, 1760–1762.
41 K. Takematsu, H. R. Williamson, P. Nikolovski, J. T. Kaiser, Y. Sheng, P. Pospíšil, M. Towrie, J. Heyda, D. Hollas, S. Záliš, H. B. Gray, A. Vlček and J. R. Winkler, *ACS Cent. Sci.*, 2019, **5**, 192–200.
42 K. Takematsu, H. Williamson, A. M. Blanco-Rodríguez, L. Sokolová, P. Nikolovski, J. T. Kaiser, M. Towrie, I. P. Clark, A. Vlček, J. R. Winkler and H. B. Gray, *J. Am. Chem. Soc.*, 2013, **135**, 15515–15525.
43 A. J. Di Bilio, M. G. Hill, N. Bonander, B. G. Karlsson, R. M. Villahermosa, B. G. Malmström, J. R. Winkler and H. B. Gray, *J. Am. Chem. Soc.*, 1997, **119**, 9921–9922.
44 S. M. Berry, M. Ralle, D. W. Low, N. J. Blackburn and Y. Lu, *J. Am. Chem. Soc.*, 2003, **125**, 8760–8768.
45 D. K. Garner, M. D. Vaughan, H. J. Hwang, M. G. Savelieff, S. M. Berry, J. F. Honek and Y. Lu, *J. Am. Chem. Soc.*, 2006, **128**, 15608–15617.
46 Z. Cai, T. Liu, Q. Lin, J. He, X. Lei, F. Luo and Y. Huang, *J. Chem. Inf. Model.*, 2023, **63**, 2936–2947.
47 Z. Cai, H. Peng, S. Sun, J. He, F. Luo and Y. Huang, *J. Chem. Inf. Model.*, 2024, **64**, 2933–2940.
48 M. Van de Kamp, R. Floris, F. C. Hali and G. W. Canters, *J. Am. Chem. Soc.*, 1990, **112**, 907–908.
49 A. F. Corin, R. Bersohn and P. E. Cole, *Biochemistry*, 1983, **22**, 2032–2038.
50 A. V. Morozov, T. Kortemme and D. Baker, *J. Phys. Chem. B*, 2003, **107**, 2075–2090.
51 R. O. Louro, T. Catarino, C. M. Paquete and D. L. Turner, *FEBS Lett.*, 2004, **576**, 77–80.
52 E. L. Mehler and G. Eichele, *Biochemistry*, 1984, **23**, 3887–3891.
53 K. K. Lee, C. A. Fitch and B. García-Moreno, *Protein Sci.*, 2002, **11**, 1004–1016.
54 J. R. Winkler and H. B. Gray, *J. Am. Chem. Soc.*, 2014, **136**, 2930–2939.
55 J. J. Warren, M. E. Ener, A. Vlček, J. R. Winkler and H. B. Gray, *Coord. Chem. Rev.*, 2012, **256**, 2478–2487.
56 J. S. Kretchmer, N. Boekelheide, J. J. Warren, J. R. Winkler, H. B. Gray and T. F. Miller, *Proc. Natl. Acad. Sci. U.S.A.*, 2018, **115**, 6129–6134.
57 N. M. Kostic, R. Margalit, C. M. Che and H. B. Gray, *J. Am. Chem. Soc.*, 1983, **105**, 7765–7767.
58 C. N. Pace, B. M. P. Huyghues-Despointes, J. M. Briggs, G. R. Grimsley and J. M. Scholtz, *Biophys. Chem.*, 2002, **101–102**, 211–219.
59 A. Bhattacherjee, S. Mallik and S. Kundu, *J. Mol. Evol.*, 2015, **80**, 10–12.
60 N. Osada and H. Akashi, *Mol. Biol. Evol.*, 2012, **29**, 337–346.